Available online at www.sciencedirect.com
SCIENCE DIRECT®
ELSEVIER
Journal of Magnetism and Magnetic Materials 293 (2005) 715–724
Journal of magnetism and magnetic materials
www.elsevier.com/locate/jmmm

Magnetically modulated optical nanoprobes (MagMOONs) for detection and measurement of biologically important ions against the natural background fluorescence of intracellular environments

Teresa Gail Roberts, Jeffrey N. Anker, Raoul Kopelman*

Department of Chemistry, The University of Michigan, 930 N. University Avenue, Ann Arbor, MI 48109, USA

Available online 25 March 2005

Abstract

Magnetically modulated optical nanoprobes (MagMOONs) have been synthesized for the detection of pH changes in intracellular environments. MagMOONs are nanosensors designed to emit fluorescent signals and to blink in response to rotating magnetic fields. Separating the blinking probe signal from the unmodulated background signal allows for simple and sensitive detection of low analyte concentrations in the presence of autofluoresence.

PACS: 82.80.−d; 81.20

Keywords: Biosensor; MagMOONs; Fluorescence; Spectroscopy; Barium ferrite; SNARF-1; pH sensor; Synthesis; Silica

1. Introduction

During the past 15 years, there has been a remarkable growth in the use of fluorescence as an analytical tool for detection and quantification of trace constituents in biological and environmental samples. Applications of fluorescence methods of analyses have spread from the traditional areas of biochemistry and biophysics into the areas of environmental monitoring [1,2], clinical chemistry [3,4], DNA sequencing [5], cell sorting (flow cytometry) [6] and genetic analysis by fluorescence in situ hybridization (FISH) [7]. The use of fluorescent tags is rapidly replacing more expensive and difficult-to-handle radioactive tags in medical tests such as enzyme-linked immunoassays (ELISA) and fluorescence polarization immunoassays [8]. The key to this phenomenal growth in

*Corresponding author. Tel.: +1 734 764 7541; fax: +1 734 936 2778.
E-mail address: kopelman@umich.edu (R. Kopelman).

0304-8853/$ - see front matter © 2005 Published by Elsevier B.V.
doi:10.1016/j.jmmm.2005.02.070

fluorescence spectroscopy is its high sensitivity and selectivity. In addition, fluorescent measurements are rapid and use relatively inexpensive and rugged instrumentation.

Limits of detection in fluorescence spectroscopy are often governed not by one's ability to induce or detect the fluorescence of an analyte, but rather the ability to distinguish analyte fluorescence from background interferences, including naturally occurring fluorophores in biological samples. Depending on the type of sample and analyte, methods exist for background correction, such as dual-laser differential fluorescence correction and phase-modulation fluorometry [9–11]. However, many of these methods are not appropriate for use in living tissue. In general, sample autofluorescence, in conjunction with background fluorescence from instrument optics, is responsible for limiting the signal-to-noise ratio and, thus, reducing sensitivity. Thus, rejecting background fluorescence and increasing signal-to-noise ratios by orders of magnitude has the potential of leading to important advances in molecular and biomedical sciences.

Since 1995, this research group has focused on the use of fluorescence spectroscopy as applied to nanotechnology. Fiber optic biosensors designed for fluorescence detection [12–14] were eventually replaced by *p*hotonic *e*xploreres for *b*ioalaysis in *b*iologically *l*ocalized *e*mbedding (PEBBLEs) [15–17] PEBBLEs consist of fluorescent dyes entrapped in a matrix composed of silica, polyacrylamide or methyl methacrylate and have been used for intracellular and in vitro measurements of ions and molecules such as Mg^{2+}, Zn^{2+}, Ca^{2+}, Na^{+}, K^{+}, H^{+}, Cl^{-}, NO^{2-}, O_2, glucose. By entrapping dye within a matrix, the cell environment is protected from toxic effects of the dye and the dye is protected from adverse affects from substances within the cytosol. PEBBLEs evolved into dynamic nanoplatforms in which were entrapped species for other functionalities, such as enzymes, iron oxide or gadolinium-DTPA, ionophores, sensitizing dyes and proteins that enable the nanoplatforms can be targeted to specific cells [18]. Dynamic nanoplatforms have been used for magnetic resonance imaging in mouse brains, drug delivery and cancer therapy. Although these nanoprobes represent significant advancement in nanotechnology, they still have not been able to resolve the issue of background fluorescence from instrument optics, and autofluorescence of biological samples.

This paper focuses on the synthesis of *mag*netically *mo*dulated *o*ptical *n*anoprobes (MagMOONs), the next generation of PEEBLEs technology. MagMOONs are novel nanosensors designed to emit a fluorescence signal and to blink in response to a rotating magnetic field [19,20]. MagMOONs are generated by vapor depositing a layer of aluminum over one hemisphere of a silica nanosphere in which is entrapped magnetic material and fluorescent dye. When a rotating magnetic field is applied to MagMOONs in solution, the microspheres rotate, seemingly passing through the phases of the moon (Fig. 1). Thus, the MagMOONs appear to blink as the light emitting side comes in and out of view. The aluminum coating prevents excitation light from entering and fluorescence from leaving the coated side of the MagMOON (Fig. 2). Subtracting unmodulated background fluorescence from the modulated MagMOON signal greatly increases the single-to-background ratio, thus enhancing sensitivity and lowering detection limits. In addition, the blinking capabilities of the magnetic nanosensors allow for the detection of analytes in the presence of naturally occurring autofluorescence of biological samples as well as fluorescently stained cells.

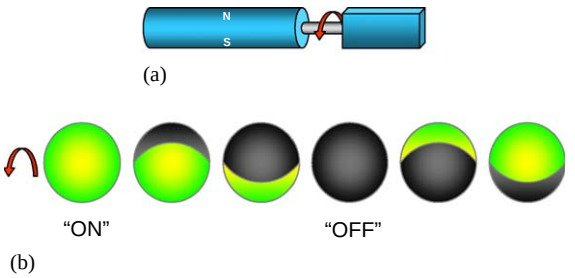

Fig. 1. (a) Graphic of rotating magnet used for rotating MagMOONs in aqueous suspension. (b) MagMOONs appearing to blink as they rotate through the phases of the moon.

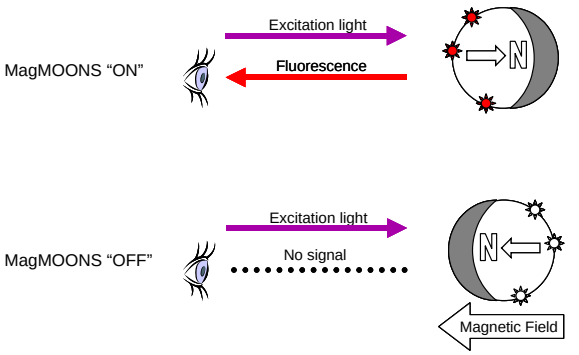

Fig. 2. MagMOONs are ON when the non-coated hemisphere is facing the detector. In this orientation fluorescent dyes are exposed to light of the appropriate excitation wavelength. The resulting fluorescent emission is allowed to reach the detector. MagMOONs are OFF when the coated hemisphere is facing the detector. In this orientation, the fluorescent dyes are protected from excitation energy and no emission signal reaches the detector.

2. Experimental

2.1. Reagents

Magnetic barium ferrite (BaM) hexagonal nanocrystals approximately 30 nm in diameter were obtained from Toda Kogyo Corporation (1-4 Meijishinkai, Otake, Hiroshima 739-0652 Japan). Dextran-linked (MW 10,000) carboxy SNARF®-1 fluorescent day was obtained form Molecular Probes, Inc. (Eugene, OR). Ethanol (reagent grade, 95.0%), ammonium hydroxide (28.0–30.0% NH_3) and tetraethyl orthosilicate (TEOS, 99 + %) were received from Aldrich (Milwaukee, WI).

2.2. MagMOON synthesis

Magnetic BaM was ground by hand for 1 h in a 10 cm diameter aluminum oxide mortar pestle. Approximately 40 mg of ground BaM was added to 10 mL solution of ammonium hydroxide and deionized water (4.33:1 v/v). The mixture was sonicated for 1 h, then centrifuged for 15 min at 500 rpm using a Marathon 21000 centrifuge (Fisher Scientific). After centrifugation, 3.84 mL of supernatant was transferred to a 100 mL round bottom flask. To this mixture were added 20.4 mL ethanol and 800 μL 0.5 mM dextran-linked carboxy SNARF®-1 dye. The polymerization reaction was initiated by adding 70 μL tetraethyl orthosilicate. The reaction was allowed to proceed for 2 h. The product was filter using vacuum filtration, rinsed with ethanol, and dried. Blank silica nanospheres were prepared using this same procedure and omitting the addition of BaM and carboxy SNARF®-1. Particle diameter was determined by imaging using a Philips CM 12 scanning transmission electron microscope.

2.3. Metal coating of silica particles

Silica nanospheres (MagMOON precursors) containing BaM and carboxy SNARF®-1 dye were coated on one hemisphere with aluminum metal using an in-house vapor deposition apparatus as illustrated in Fig. 3. The procedure is described as follows. (1) Approximately 5 mg of MagMOON precursors was dispersed in 1 mL deionized water by sonicating at 42 kHz for 30 min in a Fisher Scientific sonic bath, FS30 H. (2) A drop of the suspension was deposited on a glass microscope slide that had previously been cleaned by soaking in NoChromix® (Fisher Scientific). Cleaning the glass slide in NoChromix® reduces the surface tension between the glass and the suspension, allowing for the suspension to be spread into a thin layer rather than remaining in a tight droplet. (3) Aluminum was deposited onto the surface of the slide to a thickness of

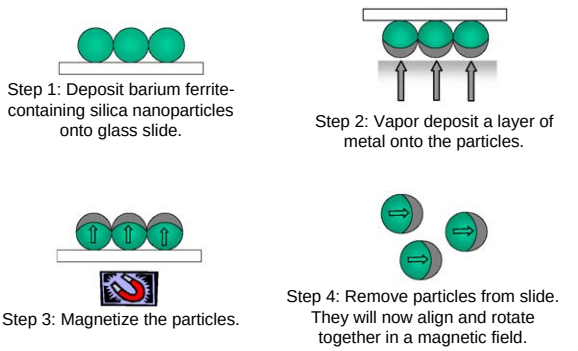

Fig. 3. Steps involved in the transformation of precursors into MagMOONs that can be oriented and rotated by a magnetic field.

approximately 20 nm. The thickness of the Al coating was monitored using a piezo-eletric thickness monitor during deposition. (4) After metal deposition, the Al coated precursors were magnetized to form MagMOONs by placing the slide in a strong magnetic field such that the uncoated hemisphere was oriented toward the north magnetic pole. (5) MagMOONS were removed from the slide by gently brushing with a soft artist's brush and sonicating the tip of the brush in buffer or other solution.

2.4. Spectra acquisition for rotating MagMOONs

MagMOONs were dispersed by sonicating in pH 5.5 and 9 phosphate buffer. A small drop of the suspension was transferred to a glass microscope slide. Single particles and aggregates were viewed using the instrumentation described above. To modulate MagMOONs, a permanent magnet was held above the microscope stage and rotated with a computer controlled stepper motor attached to the magnet. Data were collected over a time period of 141 seconds as the MagMOONs rotated to "On" and "Off" orientations. A program written in LABVIEW controlled the motor with pulses sent through a parallel port to orient the MagMOONs in "On" and "Off" orientations. Spectra were acquired and saved each time the MagMOONs were reoriented.

2.5. SQUID analysis

A superconducting quantum interference device (SQUID) was used to measure magnetic hysterisis curves for MagMOONs and pure BaM.

2.6. pH calibration curve

MagMOONs were dispersed in deionized water by soniating 10 mg MagMOONs in 1.0 mL deionized water. Certified pH buffer solutions (Fisher) ranging from pH 3 to 10 were used. A 150 μL aliquot of each buffer solution was transferred to a microwell plate (Whatman). To each aliquot was added 10 μL MagMOON suspension. Green and blue excitation light was provided by passing light from a Hg/Xe lamp through a green and blue Olympus filter cube. The particles were viewed with the 40× objective of an Olympus IMT-II (Lake Success, NY) inverted fluorescence microscope. Fluorescence emission spectra were acquired using an Acton Research Corp. spectrograph and a Hamamatsu HC230 CCD interfaced with an Intel Pentium computer in conjunction with a program written in LABVIEW (National Instruments, Austin, TX). Subsequent data processing was performed using Microsoft Excel software.

3. Results and discussion

There are four components that must be considered in the synthesis of MagMOONs: matrix composition, fluorescent dye, magnetic material and capping metal. These components are described below.

3.1. Nanoparticle matrix and particle size

This research group has synthesized nanoparticles using a variety of methods and particle matrices, including, polyacrylamide (PAA) using reverse microemulsion techniques, decyl methacrylate, and silica according to the Stöber method. PAA has been used to entrap hydrophilic dyes whereas decyl methacrylate has been used primarily for hydrophobic applications. Silica, on the other hand, has proven useful with both hydrophilic and hydrophobic dyes. Due to its amphiphillic characteristics and its ease of synthesis, a silica matrix was selected for use in the first generation of MagMOONs.

MagMOONs must be heavily loaded with fluorescent dye as well as magnetic material in order to rotate and function as anticipated. It was estimated that a particle size of 1 μm or less would prove large enough to entrap the necessary masses of dye and BaM while remaining small enough to avoid perturbing the internal environment of a mammalian cell. Stöber [21] reports that the size of silica nanoparticles synthesized by his method is controlled by the ratio of ammonia to water. Fig. 4a shows the STEM image of blank silica nanoparticles synthesized using the volume of

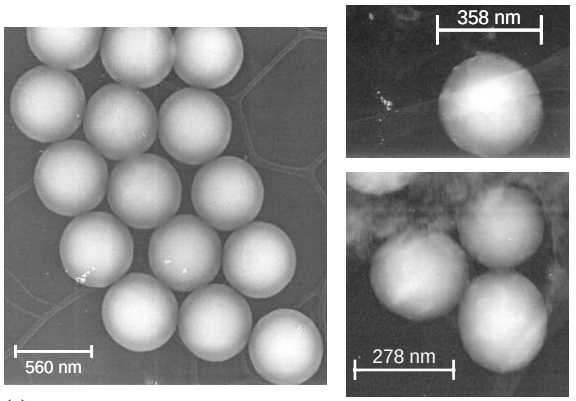

Fig. 4. (a) STEM image of blank silica nanoparticles. (b) STEM images of silica nanoparticles containing dextran-linked carboxy SNARF®-1 fluorescent dye and BaM nanocrystals.

ammonium hydroxide and water (4.33:1 v/v) described in the experimental section and 700 μL TEOS. This procedure yielded approximately 0.5 g silica particles that were approximately 560 nm in diameter. However, when dextran-linked carboxy SNARF®-1 fluorescent dye and BaM were added to the synthesis, the particle size was reduced to 275–350 nm while the yield remained the same (Fig. 4b). The decrease in particle size in the presence of 10,000 molecular weight dextran could be the result of nucleation in the presence of dextran. The MagMOON precursors shown in Fig. 4b did not have sufficient mass of BaM per particle to enable all the MagMOONs to rotate under the influence of a magnetic field. With further experimentation, is was found that by reducing the volume of TEOS used in the nanoparticle synthesis by 90% while maintaining the same ratio of ammonia to water as described in the experimental section, product yield was reduced to 25 mg. Thus, the mass of dye and BaM per particle was significantly increased due to the dramatic decrease in particle yield. Since the ratio of ammonia to water was held constant while the volume of TEOS was reduced, silica particle size remained in the 275–350 nm range regardless of the reduction in particle yield.

3.2. Choice of fluorescent dye

For initial MagMOONs studies, a fluorescent probe that exhibits changes in photophysical characteristics as a result of changes within the cytosolic pH range of 6.8 to 7.4 was selected. The fluorescent dye chosen was dextran linked 5′(and 6′)-carboxy-10-dimethylamino-3-hydroxy-spiro[7H-benzo[*c*]xanthene-7,1′(3H)-isobenzofuran]-3′-one (carboxy SNARF®-1), which is a fluorescein derivative [22]. In carboxy SNARF-1, only the phenolic group, the tertiary amine and the ortho-carboxyl group on the single lower ring structure become charged species at varying pH. The other carboxyl functional group is not critical to fluorescence output or pH response [23]. Specifically, it is the protonation/deprotonation of the phenol (pK_a ~7.5 at room temperature; pK_a ~7.3–7.4 at 37 °C) that renders carboxy SNARF-1 useful for measuring pH changes between pH 7 and 8. A distinct advantage to using carboxy SNARF®-1 for pH measurements is the flexibility offered by the fact that the dye is both dual absorptive and dual emissive (typically at 580 and 640 nm) and has a clear isosbestic point (610 nm) allowing for ratiometric measurements of fluorescent intensities at varying pH. By using ratiometric measurements for the construction of pH calibration curves, instrumental fluctuations, variations in lamp intensity and inconsistencies in concentrations are eliminated. The dextran derivative of carboxy SNARF-1 was selected for use in MagMOONs due to the fact that the large size of the dextran molecule (MW ~10,000) prevents leaching of the dye from the silica matrix. The dextran conjugate has the same pH behavior in aqueous solution as free carboxy SNARF.

3.3. Choice of magnetic material

The most important requirement of the magnetic material that is entrapped within the MagMOON matrix is that the coercivity is high enough that the material orients in a magnetic field but is not remagnetized by the applied field (if the field is stronger than the coercivity, the MagMOONs are magnetized in uncontrolled orientations, and will no longer blink in phase). To

produce strong torques required to rapidly move the MagMOONs in highly viscous solutions and cell cytoplasm, MagMOONs should have a high loading of material of high magnetization and high coercivity. The torque exerted on MagMOONs by a magnetic field is described by

$$\text{Torque} \sim MB,$$

where B is the external magnetic field strength and M is the magnetization of the particle. Rotation rates can be increased either by increasing M or increasing B. M can be increased by using higher loading of magnetic material and by using magnetic material with higher magnetization per volume. B can be increased by applying a stronger magnetic field, but the applied field must be less than the coercivity of the magnetic material in the MagMOON.

A SQUID magnetometer was used to acquire magnetic hysterisis curves for the 300 nm MagMOONs containing barium ferrite and dextran-linked carboxy-SNARF dye (Fig. 5). From the hysterisis curve, the coercivity was estimated to be ~3750 Oe, while the saturation magnetization was estimated to be 0.25 emu/g, which is approximately 0.5% by mass of the saturation magnetization for the pure BaM. This implies that the MagMOONs contained approximately 0.5% magnetic BaM nanoparticles by mass, or 0.1% by volume, assuming that the BaM had a density of 5 g/cm^3, and the dry silica matrix had a density of 1 g/cm^3. On average, a 300 nm diameter MagMOON would contain approximately four 30 nm diameter 5 nm high hexagonal BaM nanoparticles.

The magnetic fields used to orient the MagMOONs are typically 50–1000 G. In a 1000 G external field, the difference in energy between aligning the magnetic moment of a single BaM nanoparticle with the field and aligning it against the field is ~40 times larger than thermal energy at room temperature (298 k_B). Thus even for single MagMOONs containing few nanoparticles, the magnetic orientation energy is strong compared to Brownian forces.

The BaM nanoparticles are trapped within the MagMOONs with a fixed orientation in the matrix. When an external field is applied to magnetize the MagMOONs, the entrapped BaM nanoparticles are expected to magnetize along their easy axis through the height of the hexagonal nanoparticles in a direction with a positive projection onto the magnetizing vector. The net magnetization of the MagMOON is the sum of the magnetic vectors of the individual BaM particles

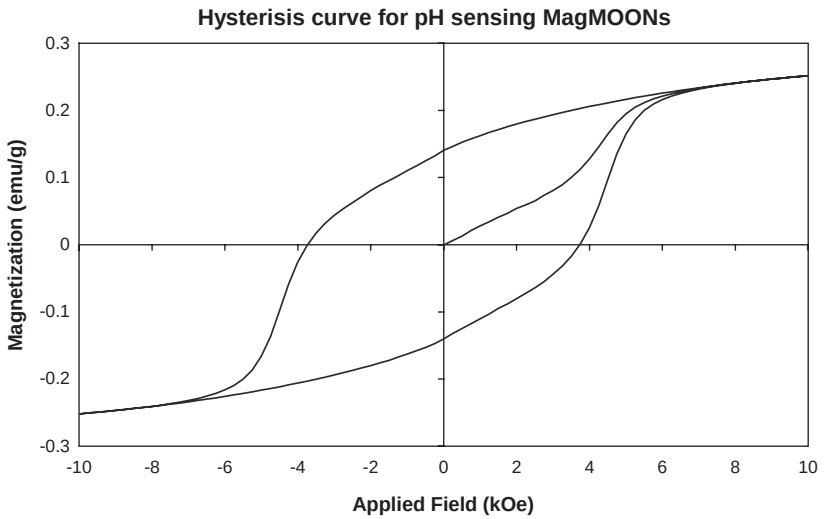

Fig. 5. Hysteresis loop obtained by SQUID analysis of 300 nm MagMOONs containing dextran-linked carboxy SNARF®-1 fluorescent dye and BaM nanocrystals.

inside. For a MagMOON containing many BaM nanoparticles, the net magnetization vector averages to point close to the orientation of the applied field, and the metal hemisphere coating aligns with the MagMOON moment. If a MagMOON contains only a single, however, the magnetization could be up to, but no more than, 90° off of the magnetizing field, and an ensemble of such particles will blink synchronously producing a strongly modulated signal, but with individual MagMOONs shifting phase ahead or behind by up to 90°. We observed that the MagMOONs produced here blinked synchronously, and produced a strongly modulated signal.

3.4. Choice of metal capping material

The metal coating deposited on one hemisphere of each MagMOON must fulfill either of two criteria (or both). It must (1) prevent excitation light from entering the coated side of the nanosphere and (2) prevent fluorescence emission from exiting the coated side. The metal layer should ideally be thicker than the skin depth of the excitation or emission light. However, thinner layers that allow a small portion of light to enter or exit the MagMOON may be acceptable as long as modulation of light between the "On" and "Off" orientations of the MagMOONs occurs. MagMOONs have been coated with vapor-deposited aluminum, sputter-coated gold [19], and molecular beam deposition (MBD) of cobalt [24]. Aluminum was chosen for coating one hemisphere of the MagMOONs synthesized in this experiment because it has a higher optical density than gold, and the vapor deposition process is simpler than MBD. Quenching of the dye by the metal is not significant since most of the dye molecules are not in immediate proximity (<10 nm) to the metal.

3.5. pH calibration curve

The spectra acquired using MagMOONs in certified buffers ranging in pH from 3 to 12 are shown in Fig. 6. The spectra have been normalized to the isosbestic point. The peaks observed at 590 nm represent the protonated form of the phenolic functional group (the acid peak), whereas the peak seen at 640 nm is attributed to the deprotonated form (the base peak) of this same functional group.

Fig. 7 illustrates the pH calibration curve that was obtained by taking the ratio of the maximum fluorescent intensity averaged over 645 to 655 nm to the isosbestic point. The linear range of this curve extends from approximately pH 6 to 10,

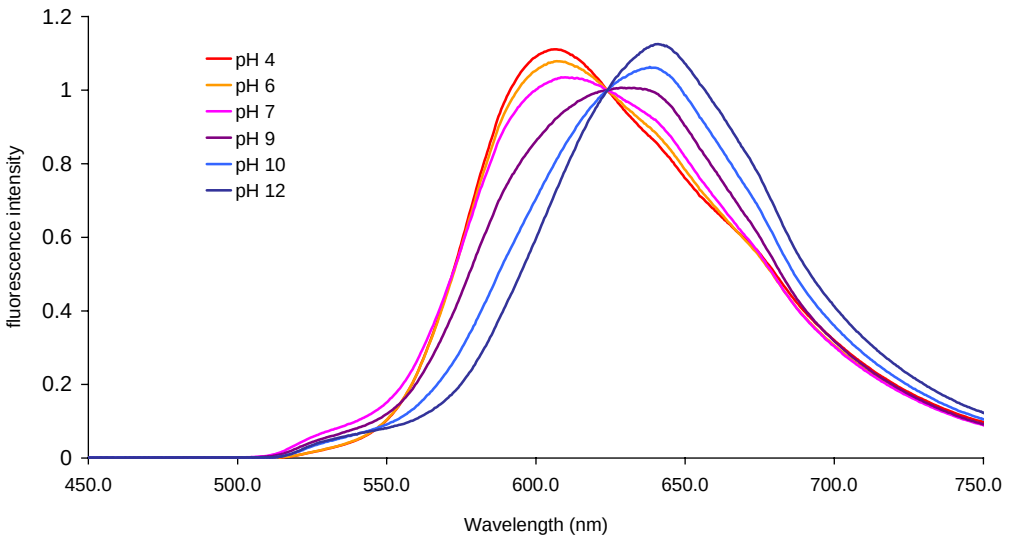

Fig. 6. Overlaid spectra of MagMOONs in pH buffers ranging in pH from 3 to 12.

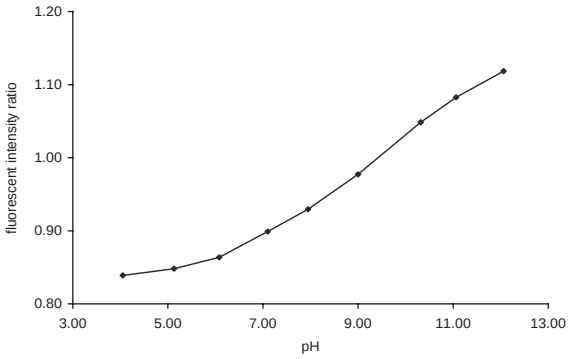

Fig. 7. pH calibration curve constructed from spectra shown in Fig. 5.

which is much broader than that of free carboxy SNARF®-1 in buffer. This broadening of the linear range is a characteristic typical of fluorescent dyes entrapped in matrices that extend the useful linear range of the dye.

Fig. 8 demonstrates the application of MagMOONs for increasing signal-to-noise ratios while overcoming background fluorescence due to variations in lamp intensities, instrumental fluctuations and autofluorescence. Fig. 8a shows the average of the ON signal and the average of the OFF signal collected over a wavelength range of 550 to 850 nm and a time period of 141 s using green excitation of MagMOONs rotating in pH 5.5 phosphate buffer. The large peaks above 725 nm come from imperfectly filtered excitation light from the Hg/Xe lamp. The inset in Fig. 8a shows the same spectra with the wavelength axis rescaled from 550 to 750 nm for clarity. Note that the spectra from the averages of the ON and the OFF signals are barely discernible slightly above the x-axis.

Fig. 8b illustrates the averages of the ON and OFF signals rescaled to a fluorescence intensity range of 0.00 to 0.20. The increase in intensity due to the lamp begins to appear at 730 nm. Fig. 8c was constructed by subtracting the average of the OFF signal from the average of the ON signal. This figure demonstrates the principle of MagMOONs: although the fluorescence intensity of the average ON minus the average OFF signal is only 0.04, which is negligible against the peak background intensity of 10 from the Hg/Xe lamp, this small signal is made visible by the modulation (blinking) of MagMOONs. One might argue that the average ON minus the average OFF signal is merely a result of photobleaching of the dye. However, the inset in Fig. 8c shows the beginning ON signal minus the ending ON signal. The fluorescent intensity axis for the inset has been rescaled from −0.001 to 0.009 so that this signal can be visualized. The inset demonstrates that photobleaching is negligible.

4. Conclusion

Magnetically modulated optical nanoprobes (MagMOONs) are novel nanosensors designed to emit a fluorescence signal and to blink in response to a rotating magnetic field. Separating the blinking probe signal from the unmodulated background signal allows for the simple and sensitive detection of low analyte concentrations even in the presence of autofluorescence and other background signals. MagMOONs promise to enhance the signal-to-noise ratio of a variety of applications based on fluorescence spectroscopy, including biomedical immunoassays, intracellular chemical sensors, cellular labels or tags, and protein folding studies. MagMOONs have the potential to extend the range of fluorescent indicator dyes into regions that have previously been difficult to manage, such as the UV region. Future work using MagMOONs will be focused on improvement in biomedical immunoassays and on monitoring of various ions and molecules within intracellular environments.

Fig. 8. (a) ON and OFF emission spectra including background from Hg lamp; inset illustrates the same spectra with the wavelength rescaled from 550 to 750 nm. (b) ON and OFF emission spectra with the fluorescence intensity rescaled from 0 to 0.20. (c) "ON minus OFF" emission spectra and bleaching spectra; inset illustrates the same spectra with the fluorescence intensity rescaled from −0.001 to 0.009 to enlarge the bleaching spectra.

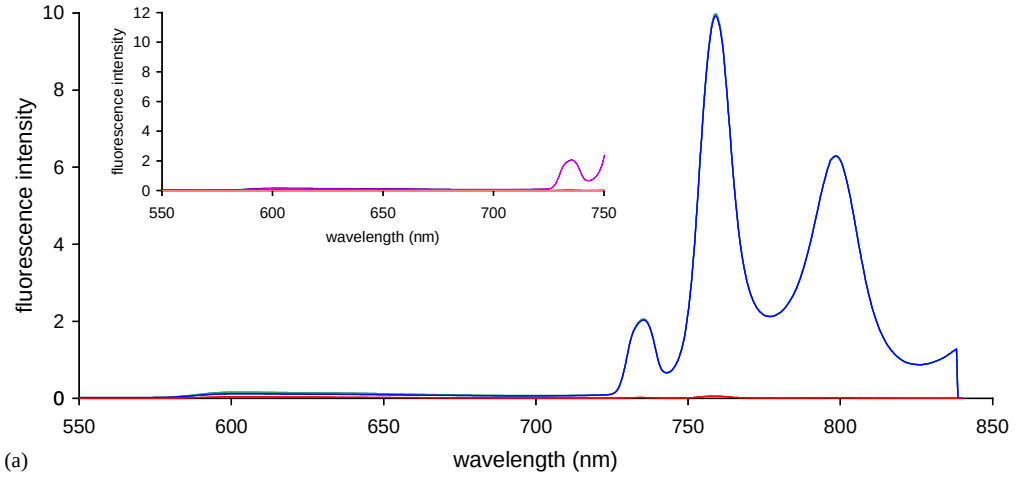
fluorescence intensity
wavelength (nm)
fluorescence intensity
wavelength (nm)

(a)

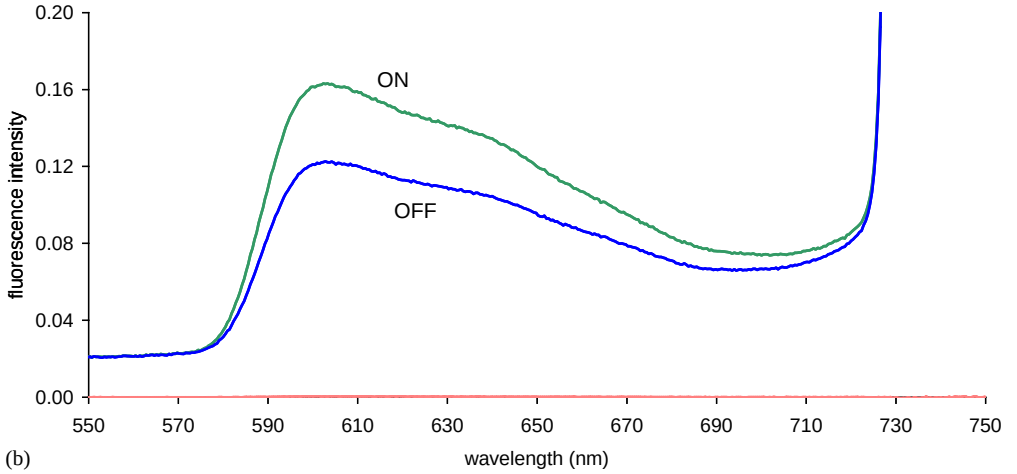
ON
OFF
fluorescence intensity
wavelength (nm)

(b)

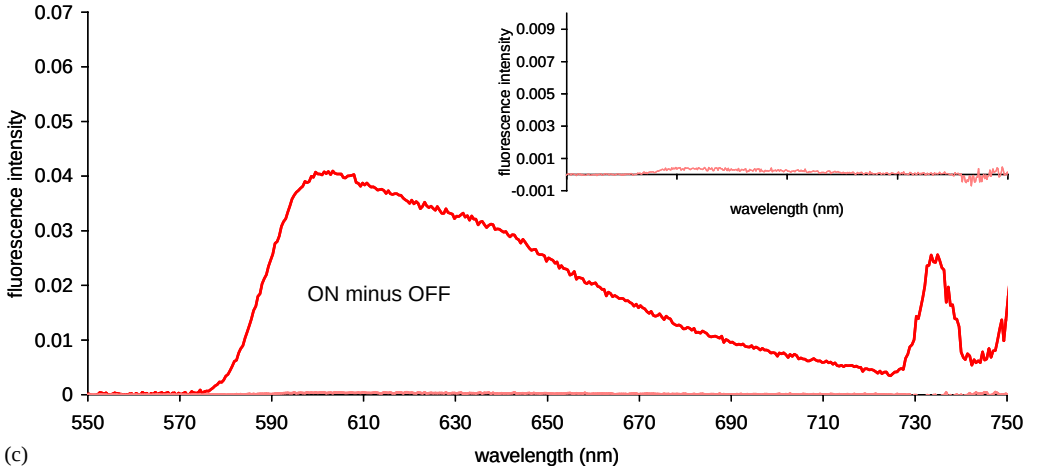
ON minus OFF
fluorescence intensity
wavelength (nm)
fluorescence intensity
wavelength (nm)

(c)

Acknowledgments

The authors gratefully acknowledge support from DARPA F49620-03-1-0297.

References

[1] U. Dorigo, X. Bourrain, A. Bérard, et al., Sci. Total Environ. 318 (2004) 101.
[2] V.N. Ivanov, J.-L. Yang, O.V. Stabnikova, et al., J. Appl. Microbiol. 96 (2004) 641.
[3] E.A. Hernández-Caraballo, L.M. Marcó-Parra, Spectrochim. Acta B 58 (2003) 2205.
[4] Q.P. Qin, O. Peltola, K. Pettersson, Clin. Chem. 49 (2003) 1105.
[5] L.-W. Lin, T.-C. Chiu, H.-T. Chang, J. Chromatogr. B 793 (2003) 37.
[6] R. Tirouvanziam, C.J. Davidson, J.S. Lipsick, et al., Proc. Natl. Acad. Sci. USA 101 (2004) 2912.
[7] E.S. Jordanova, W.E. Corver, M.J. Vonk, et al., Am. J. Clin. Pathol. 120 (2003) 327.
[8] J.R. Lakowicz, Principles of Fluorescence Spectroscopy, second ed., Kluwer Academic/Plenum Publishers, New York, 1999, p. 1.
[9] J.A. Steinkamp, C.C. Stewart, Cytometry 7 (1986) 566.
[10] H. Szmacinski, J.R. Lakowicz, Appl. Spectrosc. 53 (1999) 1490.
[11] C. Vandelest, E. Versteeg, J.H. Veerkamp, et al., J. Histochem. Cytochem. 43 (1995) 727.
[12] S.L. Barker, R. Kopelman, Anal. Chem. 70 (1998) 971.
[13] M.S. Shortreed, S. Dourado, R. Kopelman, Sensor. Actuator. B 38 (1997) 8.
[14] S.L. Barker, H.A. Clark, S.F. Swallen, et al., Anal. Chem. 71 (1999) 1767.
[15] M. Brasuel, R. Kopelman, J.W. Aylott, et al., Sensor. Mater. 14 (2002) 309.
[16] M. King, R. Kopelman, Sensor. Actuator. B 90 (2003) 76.
[17] M. Brausel, R. Kopelman, T.J. Miller, et al., Anal. Chem. 73 (2001) 2221.
[18] F. Yan, R. Kopelman, Photochem. Photobiol. 78 (2003) 587.
[19] J.N. Anker, R. Kopelman, Appl. Phys. Lett. 82 (2003) 1102.
[20] J.N. Anker, C.J. Behrend, H. Huang, et al., J. Magn. Magn. Mater., in press.
[21] W. Stöber, A. Fink, J. Colloid Interface Sci. 26 (1968) 62.
[22] J. Večeř, A. Holoubek, K. Sigler, Photochem. Photobiol. 74 (2001) 8.
[23] R.P. Haugland, Handbook of Fluorescent Probes and Research Products, ninth ed., Molecular Probes, Inc., 2002, 830pp.
[24] C.J. Behrend, J.N. Anker, et al., J. Magn. Magn. Mater. (2005), this issue.